2010 American Control Conference
Marriott Waterfront, Baltimore, MD, USA
June 30-July 02, 2010

A nonlinear approach to tracking single nanometer-scale fluorescent particles

Sean B. Andersson
Department of Mechanical Engineering, Boston University, Boston, MA 02215, sanderss@bu.edu

Abstract— **We describe a nonlinear control law for tracking single, sub-diffraction limit fluorescent particles that takes advantage of the geometric properties of the spatial intensity pattern. We present simulation results for tracking a single particle based on confocal measurements to illustrate the approach. The control law converts each intensity measurement into actuator commands directly, and consequently should yield improved temporal response over existing algorithms. We consider both two- and three-dimensional tracking.**

I. Introduction

The ability to image and analyze single molecules is a powerful tool in molecular biology that continues to be used to significantly advance knowledge of a wide-range of systems. There are a wide variety of methods yielding sub-diffraction limit position accuracy in two and three dimensions and their broad utility is evidenced by several recent review articles [1]–[3]. The main limitation of such methods is their relatively poor temporal resolution, especially when applied to systems with poor signal-to-noise ratio (SNR) such as labeled molecules inside living cells.

As a result, several alternative approaches have been developed to track a single nanometer-scale fluorescent particle. These schemes rely on point detectors in a single or multi-photon microscope. Recent reviews of the state-of-the-art can be found in [3]–[5]. Typically these schemes rely on a collection of data to estimate (directly or indirectly) the position of the fluorescent source, either by rapidly steering the laser focus around a circle [6], [7] or by using a scanning stage to acquire fluorescence measurements at different positions [8]. Other tracking approaches include [9]–[11], which track particles moving in three dimensions without scanning the focus but at expense of a more complicated detection system. Most systems are typically able to track particles diffusing with constants of 0.1-1 μm^2/s at SNRs significantly above 10, though the system reported in [7] successfully tracked quantum dots diffusing at 20 μm^2/s (though at high SNR) while [12] tracked particles with an SNR as low as 2 (though with a diffusion constant of 0.5 μm^2/s).

Servoing on the estimated position of the fluorescent particle slows down the tracking process due to the need to collect enough data for accurate estimation. In this paper we introduce an alternative scheme in which each intensity measurement is used directly in a tracking control law, without the need for the intermediate step of position estimation. This is achieved through use of a reactive control law originally developed for mapping environmental qualities such as temperature, substance concentration, and radioactivity [13], [14]. The algorithm takes advantage of the geometric features of the scalar field defined by the quantity to be mapped. Its scale-invariant nature makes it well-suited for application to systems with nanometer-scale features as evidenced by its recent application to tracking of single particles in magnetic force microscopy [15].

The process of measuring the fluorescence intensity from a single particle using a confocal microscope can be viewed as using a point-like sensor to measure a spatially and temporally varying field. The spatial field is defined by the point spread function (PSF) of a single fluorescent particle in the confocal microscope and the dynamics are governed by the motion of the particle. In this work we modify the previous tracking control law for the particular measurement scheme in the confocal setting. The resulting law steers the focal point of the microscope to converge to a periodic trajectory centered on the fluorescent particle. While the basic law is limited to tracking in the image plane, we include a preliminary approach to extend the tracking to the optical axis as well. Unlike other methods there is no explicit calculation of the position of the particle. Rather, the control law acts directly on the intensity measurements. The position of the particle can then be extracted through off-line analysis using, for example, the fluoroBancroft estimator [16].

The remainder of this paper is organized as follows. In Sec. II we describe the PSF in the confocal setting and describe how the approach takes advantage of the geometric structure. The algorithm is described in Sec. III and the simulation results are given in Sec. IV.

II. Fluorescence as a scalar potential field

In a confocal microscope, fluorescence is generated by focusing an excitation source to a diffraction-limited spot in the sample. A pinhole in the conjugate focal plane spatially filters the output light, blocking the signal arising from outside the focal volume of the microscope. A detector such as an avalanche photodiode is used to measure the output fluorescence. For a particle at the center of the focal volume of the microscope, the spatial intensity of the output fluorescence is given by

$$I(\mu,\nu) = \left(h_{\text{det}}(\mu,\nu)h^*_{\text{det}}(\mu,\nu)\right)\left(h_{\text{ill}}(\mu,\nu)h^*_{\text{ill}}(\mu,\nu)\right) \quad (1)$$

where *ill* (*det*) denotes the illumination (detection) light [17]. Here the amplitude point spread function is given by

$$h(\mu,\nu) = -i\frac{2\pi nA\sin^2\alpha}{\lambda}e^{\frac{i\mu}{\sin^2\alpha}}\int_0^1 J_0(\nu\rho)e^{-\frac{i\mu\rho^2}{2}}\rho d\rho \quad (2)$$

where n is the refractive index of the medium in which the fluorophore is embedded, $n\sin\alpha$ is the numerical aperture (N.A.) of the objective lens, A is a scaling factor, λ is the illumination or emission wavelength, J_0 is the zeroth-order Bessel function of the first kind, and (v,u) are the normalized optical coordinates given by

$$v = \left(\frac{2\pi}{\lambda} n \sin\alpha\right)\sqrt{x^2+y^2}, \quad \mu = \left(\frac{8\pi}{\lambda} n \sin^2\frac{\alpha}{2}\right) z. \quad (3)$$

The origin $(v,\mu) = 0,0$ is taken to be the center of the focal volume. With a fluorescent source at $(\Delta v, \Delta u)$ relative to the center of the focal volume, the spatial intensity is given by

$$\begin{aligned} I(\mu,v) = &(h_{\text{det}}(\mu,v)h^*_{\text{det}}(\mu,v)) \\ &\times (h_{\text{ill}}(\mu-\Delta\mu, v-\Delta v)h^*_{\text{ill}}(\mu-\Delta\mu, v-\Delta v)). \end{aligned} \quad (4)$$

The light collected by the detector, denoted I_{det}, is the integral of this function over the area of the pinhole. Due to shot noise, the actual measured signal is a Poisson process with rate I_{det} combined with the background fluorescence. It is this signal which we view as a spatial potential field.

In Fig. 1 we show simulated raster-scan images of a sub-diffraction limit sized fluorescent particle in the lateral (x,y) plane and in a plane, (x,z), along the optical axis. The parameters of the optical system were set to $n = 1.333$ to represent imaging in a water medium, an N.A. of 0.8, an excitation wavelength of 488 nm, an emission wavelength of 505 nm, and a 20 μm pinhole.

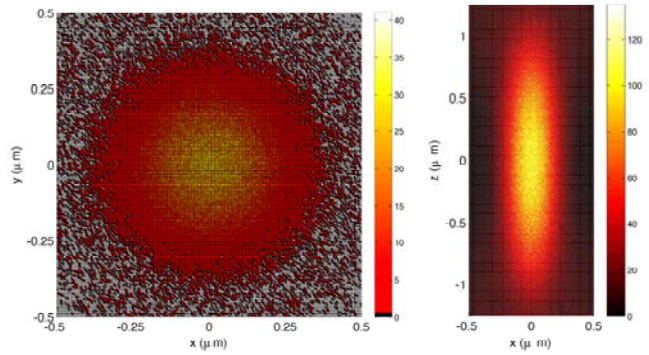

Fig. 1. Simulated confocal scan in the (left) (x,y) and (right) (x,z) planes where z is the optical axis. Simulation parameters for the optical system were N.A. = 0.8, excitation = 488 nn, emission = 505 nm, 20 μm pinhole.

III. Tracking Controller

Our goal is to develop a tracking controller which keeps the focal volume of the microscope in a region near the source particle. Actuation of the relative position between the focal volume and the particle is typically achieved in one of two ways. The first is by moving the sample while keeping the focal volume fixed. This is achieved by mounting the sample on a piezoelectric stage, allowing three dimensional motion between the particle and the focal volume. The second is by moving the focal volume with the use of actuated mirrors or acousto-optic modulators. This only allows motion in the focal plane. Motion along the optical axis is typically achieved by including a single-axis piezoelectic actuator that moves either the objective lens or the sample.

In either case, one or more piezoelectric actuators are used. These actuators, however, exhibit a variety of interesting and important dynamic effects, including nonlinearities such as creep and hysteresis, as well as cross-coupling between the axes. Such effects must be accounted for to ensure accurate control. There is a growing body of literature on efficient and effective controllers for these systems (see, e.g. [18]–[20] and discussions in [21]) and thus in this work we assume there is a low-level controller with sufficient bandwidth to drive the piezoactuators, allowing us to focus on trajectory determination. With this assumption, we can model the motion of the focal volume as

$$\dot{x} = u = \begin{pmatrix} u_x & u_y & u_z \end{pmatrix}^T. \quad (5)$$

To take advantage of the controllers developed in [13], [14], we consider first the motion of the focal volume in the plane and choose the controller form to artificially implement a nonholonomic system,

$$\begin{pmatrix} u_x \\ u_y \end{pmatrix} = v \begin{pmatrix} \cos\theta \\ \sin\theta \end{pmatrix}, \quad \dot{\theta} = v\omega. \quad (6)$$

Here the steering rate, ω, is viewed as the control input. The intensity I_{det} defines a spatial potential field. It is shown in [14] that the control law given by

$$\omega = \frac{1}{r_o}\left(1 - K\frac{d}{dt}I_{det}\right), \quad (7)$$

with the gain K sufficiently large, converges to within a distance r_o from an extremum of the potential field. Note that the time derivative is along the trajectory of the sensor (the focal point of the system in the confocal setting).

Typically, such a control would be implemented digitally. We therefore integrate (7) over a time step Δt to obtain the exact discretization

$$\theta(t+\Delta t) = \theta(t) + \frac{v\Delta t}{r_o} - \frac{vK}{r_o}\left(I_{det}(t+\Delta t) - I_{det}(t)\right). \quad (8)$$

This control law is explicitly defined by four parameters: the update rate Δt, the speed v, the gain K, and the convergence distance r_o. Implicit to the controller is the choice of an integration time on the intensity measurement. While this clearly must be less than the update rate, it should also be much shorter than the (expected) time scale of the motion of the particle to be tracked. Such a choice ensures that each intensity measurement reflects a single position of the particle rather than a sweep of positions. Shorter integration times, however, lead to lower SNR and thus this time should be chosen also with the signal and background levels in mind.

To implement tracking along the optical axis, we apply a simple proportional control law given by

$$u_z = K_z\left(I_{det}(t) - C\right). \quad (9)$$

This control law was also used in [15]. This law requires a choice of desired intensity level C. In practice, however, knowledge of the absolute intensity level is difficult to obtain.

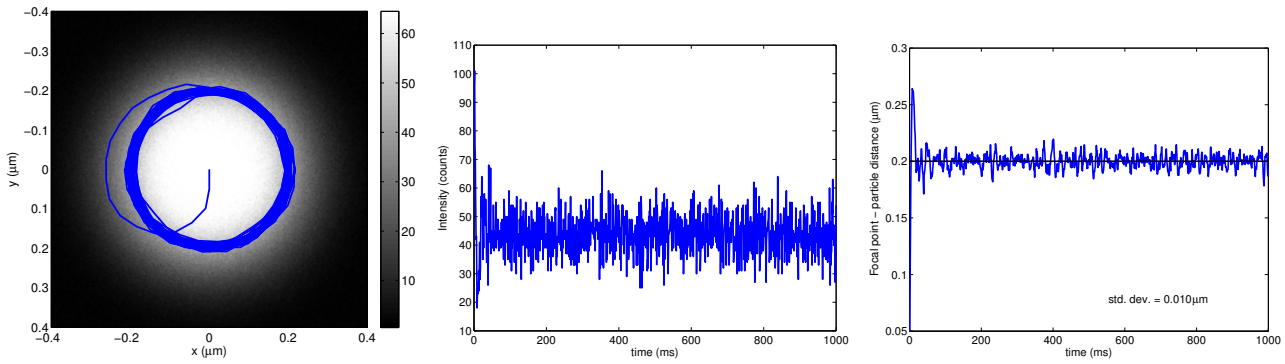

(a) Trajectory (b) Measured intensity (c) Planar distance

Fig. 2. Tracking a fixed particle. (a) The trajectory resulting from the control law superimposed upon a simulated confocal image of the spatial intensity pattern of a fluorescent particle located at the origin. Noise in the (b) measured intensity is reflected in noise in the (c) controlled distance between the center of the focal volume and the position of the fixed particle.

In addition, the choice of sign in (9) implies that reducing z will increase the intensity level. The intensity field is symmetric and thus this choice directly translates to an assumption that the particle is below the center of the focal volume. If this is violated then the control law will fail. For slowly moving particles, this assumption is not restrictive as the controller will be able to respond sufficiently fast so as to keep the focal volume above the particle. It is expected, however, that this component of the control scheme will be limiting when attempting to track faster particles. Unlike existing schemes, under the combined control law of (6), (8), and (9), each intensity measurement is used *directly* rather than being filtered through some version of position or gradient estimation.While this should allow tracking of faster particles, it is still important in application to know the trajectory of the particle itself rather than that of the focal volume of the microscope. Such estimation can be done through post-processing using a variety of methods.

IV. Simulations

To illustrate the scheme and explore the effect of parameter choices, the algorithm was simulated in Matlab. The N.A. in the simulated system was set to 0.8, the pinhole radius to 20 μm, the excitation wavelength to 488 nm, and the emission wavelength to 505 nm. The immersion media was assumed to be water and so the index of refraction was set to $n = 1.333$. The fluorescence measurements were determined by sampling a Poisson process with rate give by the integral of (4) over the area of the pinhole. The scaling factor A was set so that when the source particle was at the center of the focal volume, the intensity had a rate of 100 counts/ms.

The simulator was updated at a fixed time of 0.25 ms per cycle. Inside each cycle, the current fluorescence intensity counts was calculated and added to an accumulator. The position of the molecule was then updated according to a discrete time random walk

$$x_m(k+1) = x_m(k) + \sqrt{2D\Delta t}\, w(k) \tag{10}$$

where D was the modeled diffusion constant of the particle, Δt was the simulation update rate of 0.25 ms, and $w(\cdot)$ was a Gaussian white noise process with zero mean and unit variance. The controller update time was selected differently in different runs. At the end of each controller cycle, the total measured intensity was recorded and the position of the focal point updated according to (5) with the control given by (6), (8), and (9). In all cases r_o was set to = 0.2 μm.

We note that only shot noise was considered in these simulations. The SNR in the measurement depended upon the controller update time and upon the radius r_o since decreasing the time or increasing the radius reduced the measured intensity and since SNR typically scales as $\sqrt{N}$ where N is the number of photons measured. Intensity fluctuations also arose from the diffusive motion of the tracked particle.

A. Tracking a fixed particle

We initially simulated a particle fixed at the origin. The controller update rate was set to 1 ms, the speed was set to $v = 0.05$ μm/ms, the planar gain was set to $K = 0.05$, and the axial gain was set to $K_z = 0$ to disable motion of the focal volume along the optical axis. The focal point was initialized at the origin. The resulting trajectory, superimposed on a simulated confocal scan of the intensity, is shown in Fig. 2a. The trajectory clearly converges to a circular motion around the origin with a radius that puts the focal point relatively far away from the location of the particle. There are two main reasons for selecting a relatively large radius. The first is that in general, at a fixed speed, a larger radius circle will be easier for piezoactuators to follow than a smaller radius circle. The second is to mitigate photobleaching. All fluorescent dyes have a limited lifetime that can be understood as having a finite number of photons that can be emitted. By moving the detection volume off the particle, the particle receives a lower excitation intensity and thus the lifetime of any fluorescent dyes will be extended.

The fluorescence intensity measured along the trajectory is shown in Fig. 2b. Since the integration time was 1 ms, the mean of approximately 45 counts corresponds to a mean rate of 45 counts/ms. The corresponding SNR was 6.7. This rate is significantly lower than the expected peak intensity

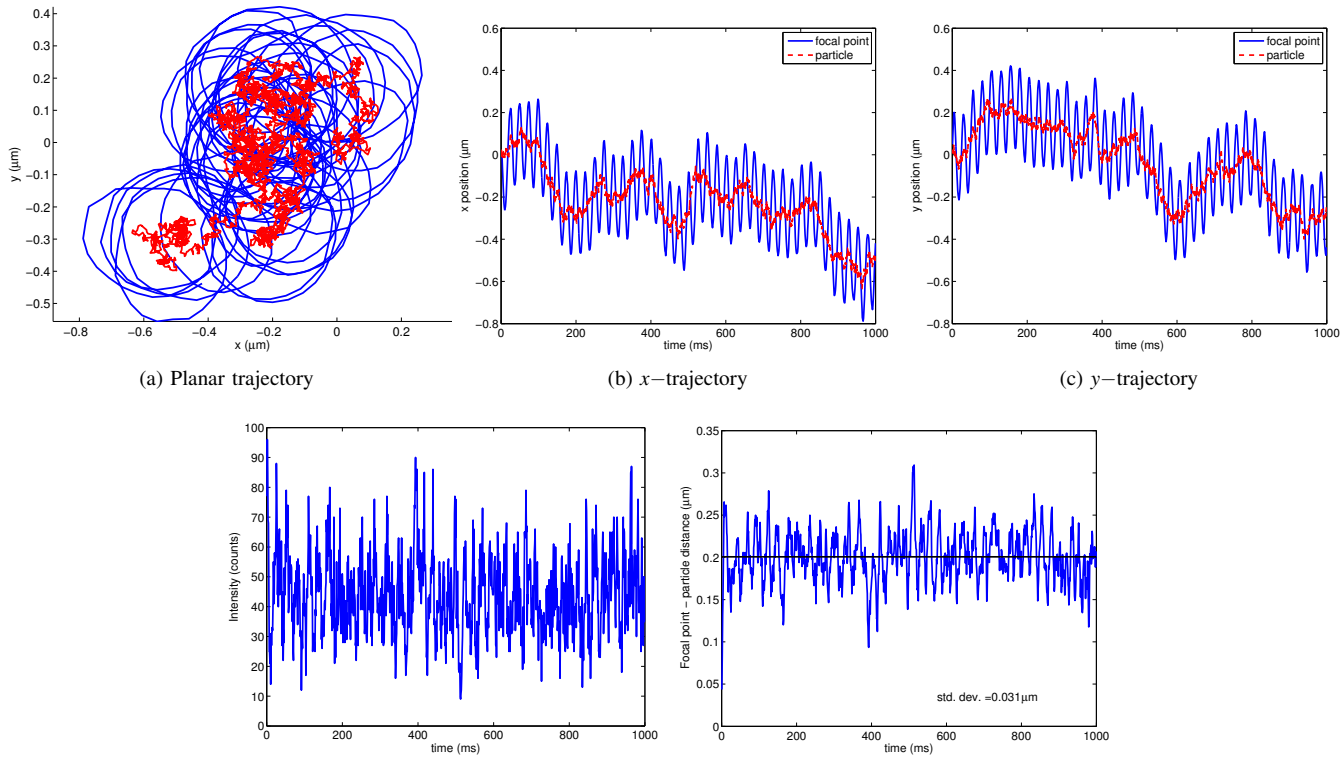

(a) Planar trajectory (b) $x-$trajectory (c) $y-$trajectory

(d) Measured intensity (e) Focal point – particle distance

Fig. 3. Simulation of planar tracking of a particle with $D = 0.1\ \mu\text{m}^2/\text{s}$. Parameters were $v = 0.05\ \mu$m/s and $K = 0.05$. It is clear from the planar trajectory and the x, y traces that the focal volume moves in a circular pattern around the particle.

rate of 100 counts/ms if the focal volume were controlled to the extremum of the intensity field, reflecting the radius that was selected for the steady trajectory. As shown in Fig. 2c, the controller quickly converged to the steady state with a small variance in the trajectory that was directly driven by the shot noise in the measurements.

B. Tracking a particle diffusing in the plane

We consider first the planar tracking law in isolation. In addition to providing intuition for the control law, there are many applications in which planar tracking is useful, such as tracking of particles moving in lipid bilayers. In addition, the planar tracking law is invariant with respect to the absolute level of measured intensity. It can thus be used even when the particle is diffusing in three dimensions so long as the particle is confined along the optical axis with a dimension smaller than the size of the PSF in that dimension (typically about 1 μm), such as occurs inside many bacterial cells.

In Fig. 3 we show a typical tracking run. The simulated diffusion constant was $D = 0.1\ \mu\text{m}^2/\text{s}$. As before the controller update time was 1 ms. The controller parameters were set to $v = 0.05\ \mu$m/s and $K = 0.05$ (with $K_z = 0$ to disable the optical axis motion of the focal volume). The planar trajectory is shown in Fig. 3a while the x and y components for both the center of the focal volume and the particle are shown in Figs. 3b,3c. The controller rate was sufficiently high that the periodic nature of the motion of the focal volume around the particle was preserved, as seen by the oscillatory nature of the focal volume trace in the x and y components.

The distance between the center of the focal volume and the particle is shown in Fig. 3d and the intensity measured along the trajectory is shown in Fig. 3e. The mean values for each are close to the fixed particle case though the variances are higher, reflecting the motion of the particle.

C. Tracking in 3-D

We then enabled particle motion and tracking in all three dimensions. The 3-D trajectory of a typical (successful) run is shown in Fig. 4 with the traces along the three axes given in Fig. 5. The particle was diffusing with a constant of $D = 0.01\ \mu\text{m}^2/\text{s}$. The parameters for the planar controller were again set to $v = 0.05\ \mu$m/s and $K = 0.05$. The gain for the vertical motion was set to $K_z = 0.001$ and the level set constant was set to $C = 40$. Note that this choice attempted to drive the vertical direction until the measured intensity level reaches 40 counts. As seen from Fig. 4 and Figs. 5a, 5b, the planar motion of the focal volume remained a circular trajectory. Fig. 5c shows that the system initially drove the focal point away from the particle and then maintained a (nearly) constant separation.

The planar distance between the focal volume and the particle along the trajectories of the run is shown in Fig. 5d while the distance along the optical axis is shown in Fig. 5e. The fluctuations in the planar distance remained relatively small, despite the larger fluctuations of the distance along the optical axis and in the intensity measurements. These

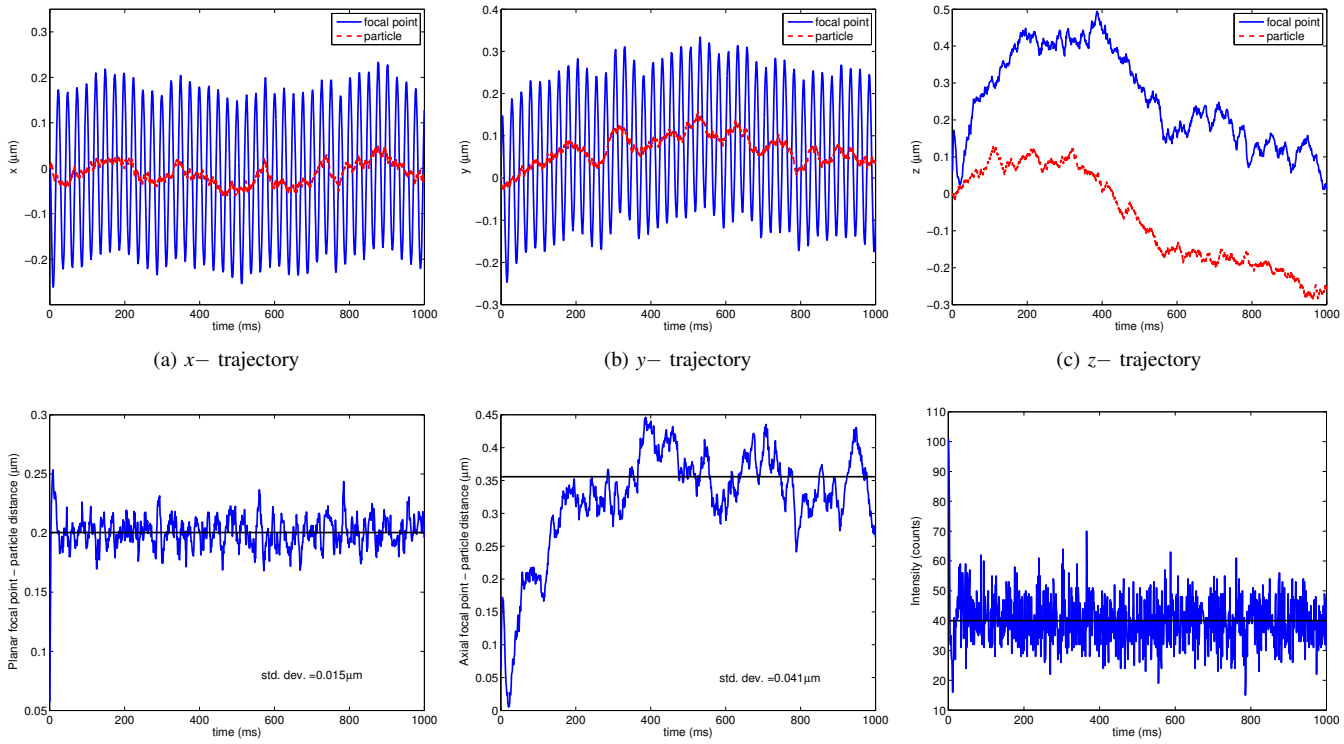

(a) $x-$ trajectory (b) $y-$ trajectory (c) $z-$ trajectory

(d) Planar distance (e) Axial distance (f) Intensity

Fig. 5. Trajectories along the (a) $x-$, (b) $y-$, and (c) $z-$ axes of the fluorescent particle and the focal volume for the motion shown in Fig. 4. The planar tracking law is independent of the motion along the optical axis and consequently its behavior is similar to the 2-D tracking results. The vertical controller drives the system to a (nearly) constant separation along the optical axis between the particle and the focal volume. The (d) planar and (3) axial distance between the focal volume and the particle reveal the relatively poor performance of the vertical controller when compared to the planar controller. The measured intensity is shown in (e).

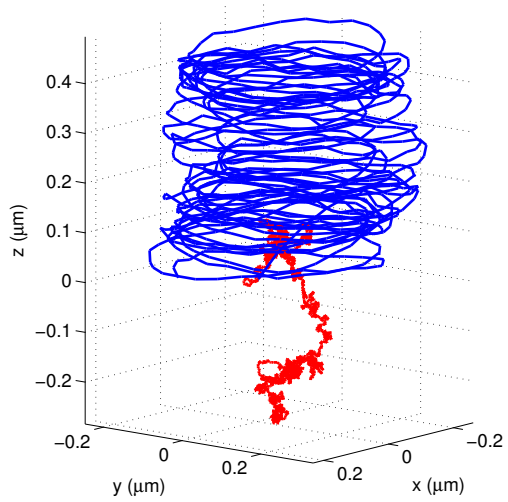

Fig. 4. Simulation of 3-D tracking with $D = 0.01\ \mu\text{m}^2/\text{s}$: 3-D trajectories of the focal volume and the fluorescent particle. Controller parameters were $v = 0.05\ \mu\text{m/s}$, $K = 0.05$, $K_z = 0.001$, and $C = 40$.

results clearly indicate that the vertical controller is not as effective as the planar law. While some improvement in the vertical performance can be achieved by increasing the gain parameter K_z, increasing it too much can lead to large overshoot. As discussed in Sec. III and illustrated below, if the focal volume moves below the particle then the controller will fail due to the symmetry of the intensity field.

To illustrate this possibility, we performed a simulation where all parameters were kept the same except for setting $C = 80$. This value was close to the expected maximum of 100 and thus the system attempted to drive the focal volume near to the particle. The particle quickly diffused above the focal plane. Once this occured, the focal volume was driven away from the particle by the controller. This was because z should have been increased to bring the particle and the focal volume closer together, thus increasing the intensity. The controller, however, assumed that decreasing the value of z would yield increasing intensity. This switch in sign caused the system to drive the focal volume away from the particle.

D. Tracking performance

Due to difficulties with the axial component of the tracking law, and the importance of planar tracking by itself, we restricted our simulation study of the performance to the tracking component only. We defined tracking performance as the standard deviation in the distance between the focal volume and the particle. To explore this performance as a function of the diffusion coefficient, we hand-tuned the controller parameters for two different controller update rates (1 ms and 0.25 ms). The results are shown in Fig. 6. Note

that when tracking was lost, the error was arbitrarily set to a value of 5. At very low values of the diffusion coefficient, the slower controller exhibited better performance. This directly reflects the increased SNR in the measurement for the longer update time. As the diffusion coefficient was increased, the error due to the motion of the particle began to dominate, eventually leading to loss of tracking. The slower controller sucessfuly tracked particles moving with diffusion coefficients of 0.7 μm^2/s while the faster controller was successful up to 2.0 μm^2/s. We note that, as expected, a four-fold increase in the controller rate yielded an approximately two-fold increase in tracking capability.

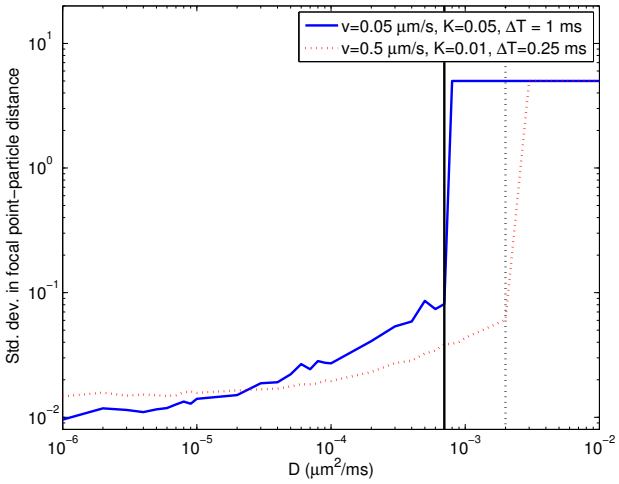

Fig. 6. Std. dev. in focal point-particle distance under two sets of controller parameters. The controller update rates were 1 ms and to 0.25 ms while the controller parameters were hand tuned. At low values of D, the increased SNR of the slower controller provides better performance while the faster controller is able to track faster particles.

Both the error and the limiting diffusion coefficient are driven in part by the SNR. The SNR can be increased by increasing the fluorescence rate of the particle (by increasing the excitation intensity), though at the cost of decreasing the time to photobleaching, and by reducing the radius of the steady-state trajectory, though at the cost of a more challenging trajectory for the focal volume. In comparison to [7], which showed tracking of diffusion rates of 20 μm^2/s, these simulations utilize a intensity levels approximately three times smaller and an integration time 10 times shorter.

V. Conclusions and Future Work

We have described a nonlinear control law for planar tracking of a diffusing fluorescent particle in a confocal fluorescence microscope combined with a linear control law for tracking along the optical axis. Simulation results indicate the planar control law is a promising alternative to existing schemes, though more work is needed for full 3-D tracking. Further study of the effect of the controller parameters on tracking performance, as well as physical implementation planned.

Acknowledgments

The author is grateful to D. Baronov for help with the simulations in Matlab. This work was supported in part by the NSF through grants DBI-064983 and CMMI-0845742.

References

[1] E. J. G. Peterman, H. Sosa, and W. E. Moerner, "Single-molecule fluorescence spectroscopy and microscopy of biomolecular motors," *Ann. Rev. Phys. Chem.*, vol. 55, pp. 79–96, 2004.

[2] E. S. Yeung, "Dynamics of single biomolecules in free solution," *Ann. Rev. Phys. Chem.*, vol. 55, pp. 97–126, 2004.

[3] W. E. Moerner, "New directions in single-molecule imaging and analysis," *Proc. Natl. Acad. Sci. USA*, vol. 104, no. 31, pp. 12 596–12 602, July 2007.

[4] N. G. Walter, C.-Y. Huang, A. J. Manzo, and M. A. Sobhy, "Do-it-yourself guide: how to use the modern single-molecule toolkit," *Nat. Meth.*, vol. 5, no. 6, pp. 475–489, June 2008.

[5] H. Cang, C. S. Xu, and H. Yang, "Progress in single-molecule tracking spectroscopy," *Chem. Phys. Lett.*, vol. 457, no. 4-6, pp. 285–291, May 2008.

[6] V. Levi, Q. Ruan, and E. Gratton, "3-D particle tracking in a two-photon microscope: application to the study of molecular dynamics in cells," *Biophys. J.*, vol. 88, no. 4, pp. 2919–2928, April 2005.

[7] K. McHale, A. J. Berglund, and H. Mabuchi, "Quantum dot photon statistics measured by three-dimensional particle tracking," *Nano Lett.*, vol. 7, no. 11, pp. 3535–3539, November 2007.

[8] Z. Shen and S. B. Andersson, "Tracking multiple fluorescent particles in two dimensions in a confocal microscope," in *Proc. IEEE Conference on Decision and Control*, 2009, pp. 6052–6057.

[9] H. Cang, C. M. Wong, C. S. Xu, A. H. Rizvi, and H. Yang, "Confocal three dimensional tracking of a single nanoparticle with concurrent spectroscopic readouts," *Appl. Phys. Lett.*, vol. 88, no. 22, pp. 223 901(1–3), May 2006.

[10] H. Cang, C. S. Xu, D. Montiel, and H. Yang, "Guiding a confocal microscope by single fluroescent nanoparticles," *Opt. Lett.*, vol. 32, no. 18, pp. 2729–2731, September 2007.

[11] G. A. Lessard, P. M. Goodwin, and J. H. Werner, "Three-dimensional tracking of individual quantum dots," *Appl. Phys. Lett.*, vol. 91, no. 22, p. 224106, November 2007.

[12] N. P. Wells, G. A. Lessard, and J. H. Werner, "Confocal, three-dimensional tracking of individual quantum dots in high-background environments," *Anal. Chem.*, vol. 90, no. 24, pp. 9830–9834, December 2008.

[13] D. Baronov and J. Baillieul, "Reactive exploration through following isolines in a potential field," in *Proc. American Control Conference*, 2007, pp. 2141–2146.

[14] ——, "Autonomous vehicle control for ascending/descending along a potential field with two applications," in *Proc. American Control Conference*, 2008, pp. 678–683.

[15] D. Baronov and S. B. Andersson, "Controlling a magnetic force microscope to track a magnetized nanosize particle," *IEEE Trans. Nano.*, to appear, 2009.

[16] S. B. Andersson, "Localization of a fluorescent source without numerical fitting," *Opt. Exp.*, vol. 16, no. 23, pp. 18 714–18 724, November 2008.

[17] J. E. Jonkman and E. H. K. Stelzer, *Confocal and two-photon microscopy. Foundations, applications, and advances*. Wiley-Liss, 2002, ch. 5. Resolution and Contrast in Confocal and Two-photon microscopy, pp. 101–125.

[18] D. Croft, G. Shed, and S. Devasia, "Creep, hysteresis, and vibration compensation for piezoactuators: atomic force microscopy application," *J. Dyn. Sys., Meas., and Contr.*, vol. 123, no. 1, pp. 35–43, March 2001.

[19] Y. Wu and Q. Zou, "Iterative control approach to compensate for both the hysteresis and the dynamics effects of piezo actuators," *IEEE Trans. Contr. Sys. Tech.*, vol. 15, no. 5, pp. 936–944, September 2007.

[20] D. Y. Abramovitch, S. Hoen, and R. Workman, "Semi-automatic tuning of PID gains for atomic force microscopes," in *Proc. American Control Conference*, 2008, pp. 2684–2689.

[21] D. Y. Abramovitch, S. B. Andersson, L. Y. Pao, and G. Schitter, "A tutorial on the mechanisms, dynamics and control of atomic force microscopes," in *Proc. American Control Conference*, 2007, pp. 3488–3502.